NETJOURNALS

Physico-chemical exploration of pesticide (imidacloprid)-induced osteoporosis in female rats and the protective effect of *Urtica urens* L. leaves

Massara Mzid[1], Hafed El Feki[2]*, Hassane Oudadesse[3], Bertrand Lefeuvre[3] and Tarek Rebai[1]

[1]Laboratory of Histo-embryology and Cytogenetics, Medicine Faculty of Sfax University, Sfax, Tunisia.
[2]Laboratory of Sciences Material and Environment, Faculty of Sciences of Sfax, B.P. 1171, 3000, Sfax, Tunisia.
[3]UMR CNRS 6226, University of Rennes 1, Campus de Beaulieu, 35042, Rennes, France.

ABSTRACT

The toxic effect of imidacloprid (IMI)-induced osteoporosis and the protective effect of *Urtica urens* L. (UU), dwarf nettle was investigated against this toxicity in female rats. Rats were divided into control group, 2 groups treated with IMI at 50 and 300 mg/kg/day, 1 group treated with 100 mg/kg/day of UU and 2 groups co-treated with IMI (50 and 300 mg/kg/day) +100 mg/kg/day of UU. The effects of IMI and UU on the bone were analyzed using five physicochemical techniques: Fourier transform infrared (FTIR) spectroscopy, X-ray diffraction (XRD), Scanning electron microscopy (SEM), dispersive X-ray spectroscopic (EDX) and biochemical analyses (Calcium and Phosphorus). Results show that IMI caused osteoporosis in female rats by a decrease in Calcium (Ca) and Phosphorus (P) levels. XRD showed that there is a moving of peaks in IMI-treated rats when compared to controls and FTIR showed also a moving of bands with IMI. SEM analysis revealed a phenomenon of textural alteration in IMI-treated groups and EDX showed a Ca/P ratio less than 1.67. UU injection ameliorated all parameters cited above. The data obtained from XRD revealed a return of peaks to their initial position for the groups treated with IMI + UU and the data obtained from FTIR showed a displacement of -CH^2, PO_4^{3-} and CO_3^{2-} bands at their initial positions. In addition, the results of SEM show that the groups treated with (IMI + UU) have normal bones compared to those treated with IMI. The Ca/P ratio increases to reach 1.8. In conclusion, this study showed that the toxicity of induced osteoporosis and the injection of *UU* have alleviated this disturbance in female rats.

Keywords: Osteoporosis, imidacloprid, bone, *Urtica urens* L., XRD, FTIR, SEM.

*Corresponding author. E-mail: Hafedelfeki@yahoo.com.

INTRODUCTION

Bone is a metabolically active calcified tissue in constant remodeling (Glimcher, 1998). It is composed of an organic matrix (mainly collagen type I (>90%) and a mineral component (nanocrystalline carbonate hydroxylapatite) in proportions varying with age and location within the skeleton. Stoichiometric apatite has a calcium to phosphorus molar ratio of 1.67, while bone mineral is slightly lower mainly due to ionic substitution (Na, Mg, HPO_4 (acid phosphate), and CO_3 ions). As bone matures, bone mineral becomes more crystalline, its calcium to phosphorus ratio increases and its content of carbonate and acid phosphate decreases. Also, there is a progressive decrease in the rate of bone turnover with age. Consequently, the proportion of mature and well-crystallized mineral to newer, less crystalline, mineral varies with time and also with health condition (Glimcher, 1998; Boskey et al., 2005).

Bone mineralization is regulated by a complicated array of feedback processes which can be altered by different genetic, endocrine, and environmental factors, resulting in abnormal or pathological composition of bone (Glimcher, 1998; Boskey et al., 2005). Thus, there is an

increasing interest in medical (Glimcher, 1998; Boskey et al., 2005) and toxicological research related to the factors that alter bone mineralization (Wang et al., 2019; Ronis et al., 2019; Li et al., 2019). From toxicology studies, it is well-known that environmental pollutants (e.g., heavy metals, organochlorines) cause skeletal defects and malformations in laboratory models and wild animals (Baxley et al., 1981).

Mineral features such as crystallite size and perfection (crystallinity), phosphate content, carbonate content, and mineral environment may be altered substantially as a function of tissue type, age, and pathology. Bone diseases such as osteogenesis imperfecta (Camacho et al., 1999), osteomalacia (Boskey et al., 1988), osteoporosis (Mzid et al., 2017), osteopetrosis (Boskey and Marks, 1985), and osteoarthritis (Miller et al., 1999) are characterized by abnormal tissue mineral content, deposition, and/or turnover.

Techniques traditionally used to study bone tissue, namely X-ray diffraction and Fourier transform infrared (FTIR) spectroscopy, while permitting identification of the nature of the mineral phases present, provide neither spatially-resolved analysis of the various mineral phases, nor permit determination of the relative amounts of mineral and matrix present (Boskey et al., 1992).

Several analytical techniques are available to assess changes in bone composition (Olszta et al., 2007). Fourier transform infrared (FTIR) spectroscopy is particularly useful as it provides detailed qualitative and quantitative information about the molecular constituents of bone (e.g., carbonate, collagen and phosphate: (Boskey et al., 2005). In this sense, infrared spectroscopy has been used to identify abnormal mineral composition caused by different pathological conditions affecting bone (Álvarez-Lloret et al., 2014). In this perspective, the use of FTIR allows a better and more detailed comprehension of changes in mineralized tissues associated with different bone disorders related with exposure to pollutants.

Imidacloprid (IMI), one of the earliest and most commonly used neonicotinoid insecticides, with characteristics of high activity, wide insecticidal spectrum, and novel insecticidal mechanism, and has been favored by the international market (Casida and Durkin, 2013; Jeschke et al., 2010). However, with the wide application of IMI, consumers are wary of the dangers of the chemical (Sibiya et al., 2019). Studies have shown that, in addition to destroying the central nervous system of pests (Rawi et al., 2019), IMI can also cause damage to other tissues and organs through oxidative stress and inflammation (Duzguner and Erdogan, 2010; Emam et al., 2018). The liver is an important metabolic organ of animals which is easily attacked by a toxic substance (Mahajan et al., 2018). It was reported that long-term exposure to IMI caused histopathological changes in the liver (Lv et al., 2019; Vohra et al., 2014). In our study, we hypothesized that IMI-induced osteoporosis (using biological methods) is caused by oxidative stress (Mzid et al., 2017).

Urtica urens (UU), which belongs to the family of *Urticaceae* and commonly known as nettle apple has been used extensively as a traditional medicine in many countries (Randall, 2003) for the treatment of anemia, rheumatism and arthritis, eczema, asthma, urinary gravel, stomach complaints, skin infections and as an anti-haemorrhagic (Arslan et al., 2014).

Furthermore, *Urtica urens* is reported by an antioxidant and antibacterial effects (Keles et al., 2001; Toldy et al., 2005). The constituents of UU include caffeoylmalic acid, flavonoids, chlorogenic acid, gallic acid and caffeic acid which are well known for their therapeutic properties (Frank et al., 1998; WHO, 2002). The main medicinal uses of nettles historically were internally as a tonic and highly nutrient food (Barnes et al., 2002). In our study (Mzid el al., 2017), we hypothesized that UU has a protective effect against IMI-induced osteoporosis in female rats. So, in this study, we will demonstrate, using physicochemical methods that IMI induces osteoporosis in rats and that UU has a protective effect against this pesticide.

We have evaluated the protective effect of UU against the toxicity of IMI. UU is one of the best medicinal plants adapted to our time, the components of its leaves are essential to maintain good health. These components are rich in vitamins (D, C), minerals (Calcium, Phosphorus, etc) and amino acids (Mzid et al., 2017). This plant is very useful for relieving arthritic and rheumatic pains, which make us think of its direct effect on bone metabolism (Doukkali et al., 2015).

The present work focuses on the *in vivo* IMI produced skeletal damage and bone remodeling disturbance, using different techniques. In addition, this study investigates the chemoprotective role of *Urtica urens* L. against toxicity effect of IMI in female rats.

MATERIALS AND METHODS

Chemicals

Confidor® 200 OD, 1[(6-chloro-3-pyridinyl) methyl]-N-nitro-2-imidazolidinimine, [CAS No. 138261-41-3], is an insecticide manufactured by Bayer CropScience (Lyon, France) and has as an active ingredient IMI in the concentration 200 g/L, was obtained from agricultural products company in Sfax, Tunisia.

Plant preparation

Urtica urens L. leaves were collected from region in Sfax-Tunisia and identified by Professor Mohamed Chaieb from the Faculty of Sciences of Sfax (Laboratory of Biology and Vegetable Ecophysiology, Faculty of Science, 3038 Sfax, Tunisia). The voucher of sample was deposited at The National Botanical Research Institute Tunisia (INRAT). It was washed with distilled water and then dried at room temperature for 2 days, afterwards, crushed, milled in a knife mill to obtain 50 g of *Urtica urens* powder and subsequently stored in glass bottles at room temperature.

The powder was extracted by using maceration with ethanol. In the maceration, method, 50 g of the powder was macerated in 1L

ethanol (volume fraction is 70%) for 3 days and subsequently, the solution is filtrated and concentrated in a rotary evaporator at 50°C.

LC–MS/MS analysis (liquid chromatography tandem mass spectrometry)

LC–MS/MS analysis of the UU ethanolic extract was carried out using an Agilent 1100 LC system consisting of degasser, binary pump, auto sampler, and column heater. The column outlet was coupled to an Agilent MSD Ion Trap XCT mass spectrometer equipped with an ESI ion source. Data acquisition and mass spectrometric evaluation were carried out in a personal computer with Data Analysis software (Chemstations). For the chromatographic separation, a Zorbax 300 Å Extend-C-18 Column (2.1×150 mm) was used. The column was held at 95% solvent A (0.1% formic acid in water) and 5% solvent B (0.1% formic acid in acetonitrile) for 1 min, followed by an 11 minutes step gradient from 5% B to 100% B, then it was kept for 4 min with 100% B, finally, the elution was achieved with a linear gradient from 100% B to 5% B for 2 min. The flow rate was 200 µl/min and the injection volume was 5 µl. The following parameters were used throughout all MS experiments: for electrospray ionization with positive ion polarity the capillary voltage was set to 3.5 kV, the drying temperature to 350°C, the nebulizer pressure to 40 psi, and the drying gas flow to 10 L/min. The maximum accumulation time was 50 min, the scan speed was 26,000 m/z/s (ultra scan mode) and the fragmentation time was 30 min.

The phenolic compounds were identified using a combination of high performance liquid chromatography (HPLC) with diode array detection and liquid chromatography with atmospheric pressure chemical ionization mass spectrometry (ESI-LC/MS/MS) on the basis of their ultraviolet (UV) spectra, mass spectra and by comparison of the spectra with those of available authentic standards.

Animals

48 mature female rats (10 to 12 weeks old), weighing about 100 g, were purchased from SIPHAT Institute of Tunis. Animals were bred and kept in our animal facility under strict hygienic conditions and were free of major pathogens. Local vivarium conditions were controlled: temperature (24°C), humidity (30 to 60%), and light (12 h: 12 h light:dark cycle). Animals were provided standard laboratory diet (MEDIMIX, Sfax, Tunisia). They were housed per group, eight per cage. The experimental protocols were conducted in accordance with the guide for the care and use of laboratory animals issued by the University of Sfax, Tunisia, and approved by the Committee of Animal Ethics (Protocol no. 94-1939, December 2014).

Experimental design

Females rats were divided into 6 groups (n = 8) as follow:

Group 1: control (did not receive any of the substances) (Mzid et al., 2017);
Group 2: received 50 mg/kg BW of IMI;
Group 3: received 300 mg/kg BW of IMI;
Group 4: received 100 mg/kg BW of UU;
Group 5: as group 2 and co-treated with 100 mg/kg BW of UU;
Group 6: as group 3 and co-treated with 100 mg/kg BW of UU.

The period of treatment was 60 days following the procedures suggested by Bouafou et al. (2007). The IMI was given by oral administration. These doses (50 and 300 mg/kg) were chosen according to the works of Eiben and Kaliner (1991); Eiben and Rinke (1989). The UU were given by intraperitoneal injection at 100 mg/kg BW (Nassiri-Asl et al., 2009).
Those doses were given once a day in the morning.

Euthanasia

The animals were sacrificed under anaesthesia by an intraperitoneal injection of imidazolan and ketamine. The blood was obtained from heart puncture. The right distal femurs were shared; their lengths were measured. Subsequently, an incision was made parallel to the long axis of the femur after dividing the fascia and the Musculus biceps femoris. All the experiments were approved by the local Ethical Committee for animal experiments.

The bones of the different groups have been ground to a powder which will be characterized with physico-chemical techniques.

Instrumental analysis procedures

Several physico-chemical techniques were employed to characterize all powders after treatment.

Determination of calcium and phosphorus bone contents

The chemical composition of the bone compound synthesized here was determined from titrations by complexometry for the determination of the calcium content, by spectrophotometry for the total phosphate content (determination of the sum of PO_4^{3-} and HPO_4^{2-} ions, using the phospho-vanado-molybdenic method (Gee and Dietz, 1953) and by coulometry (UIC, Inc. CM 5014 coulometer with CM 5130 acidification unit) for the carbonate content.

X-ray powder diffraction

X-ray diffraction patterns were recorded on Philips PW 3710 diffractometer, using Cu-Kα radiation. The samples were ground to obtain a relatively uniform particle size, placed into an aluminum sample holder and scanned in 0.05° intervals between 20° and 37° (2Ɵ) using Ni-filtered Cu-K$_α$ radiation with a minimum of 8000 counts/interval.

Infrared spectroscopy

Fourier transformed infrared absorption spectroscopy (FTIR) (Bruker Equinox 55) was used to identify the chemical links in the structure of materials.

KBr pellets were prepared by mixing 10 mg of bone powder with 500 mg of KBr in a mortar and pestle and pressing the pellet in a 13 mm KBr pellet die (McCarthy Scientific Co., Fullerton, CA). FTIR spectra were collected on a Nicolet Magna 560 FTIR instrument equipped with a KBr beamsplitter and DTGS-polyethylene detector.

Scanning electron microscopy (SEM) characterization

Bones were analyzed by SEM, using a JEOL JSM 6301F (Tokyo, Japan). Polymethylmethacrylate embedded specimens obtained from the histological preparations were mounted on the SEM. Quantification for calcium (Ca, mol%), phosphorus (P, mol%) and magnesium (Mg, mol%) was determined by wavelength dispersive X-ray spectroscopic (EDX), the ratio of calcium to phosphorus (Ca/P) was calculated by dividing the values obtained from calcium (mol%) and phosphorous (mol%) at each point.

Statistical analysis

All data are expressed as mean value ± standard errors mean (SEM). Statistical analysis was performed using one-way ANOVA followed by Tukey's post hoc multiple comparison tests using statistical software package SPSS (SPSS Inc, Chicago, IL, USA).

RESULTS

Calcium and phosphorus bone contents

Exposure to IMI modified the mineral composition of the bone. Indeed, a decrease of calcium (17.06 and 22.31%, respectively for 50 mg/kg IMI and 300 mg/kg IMI) and phosphorus (19.98 and 54.44%, respectively for 50 mg/kg IMI and 300 mg/kg IMI) in the femurs was observed in the IMI-treated groups compared to control. It is noted that this decrease is more pronounced when the dose of IMI increases. UU injection resulted in an increase of calcium (5.16%) and phosphorus (12.63%) in the 100 mg/kg UU group compared to control and a moderation of this disorder for each of (IMI+UU)-treated groups in order of (5.32, 20,96%, respectively for 50 mg/kg IMI+ 100 mg/kg UU and 300 mg/kg IMI+100 mg/kg UU) for calcium and (9.86, 58.77%, respectively for 50 mg/kg IMI+UU and 300 mg/kg IMI+100 mg/kg UU) for phosphorus (Table 1).

XRD analysis

The diffraction patterns of hydroxyapatite (HAP) and control femur are presented as a reference for evaluating the effect of the pesticide and plant (Figure 1). After 60 days of treatment, the XRD shows characteristic peaks of hydroxyapatite crystals at about 26, 32, 40, 46.7, 50, 53 and 64° (2θ). These peaks correspond respectively to the reflections of the (002), (211), (310), (222), (213), (004) and (304) planes of hydroxyapatite crystals (Figure 1).

Our study (Table 2) showed that there are displacements at the level of the values of peaks. Indeed, the presence of IMI reduces the values of Ө of the peaks 002, 211 and 310. When Ө decreases, the crystallographic parameters (a = b, c) increase, IMI consequently increases the crystallographic parameters thus inflating the crystalline mesh of the bone. The addition of UU with its intake of minerals (Ca and P) has no influence on the mesh for the high dose in IMI (300 mg/kg), which is not the case for the low dose (50 mg/kg) which showed an increase in the value of Ө thus decreasing the volume of the mesh to return to the normal state.

Infrared micro-spectroscopy

The FTIR spectra of the powder collected from the femurs of control and treated rats with IMI, IMI+UU or UU were presented in Figure 2.

In all groups, we noted the presence of characteristic bands at 2926, 1380 and 665 cm^{-1}, which are attributed to the asymmetric and symmetric bending vibrations of methylene group (CH_2). The presence of these bands is due to the existence of the -CH_2 group within the bone (Figure 3a) and which are brought in the case of the IMI-treated groups (Figure 3b). The determination of the number of waves of these bands (Table 3) clearly shows a disturbance through the treatment with IMI.

Thus, we find on the set of these spectra the bands which correspond to the modes of vibrations of the group PO_4^{3-}, observed at 565, 603, 961 and 1000 cm^{-1}. There are displacements in the values of the number of waves in the IMI-treated groups compared with the control (Table 3).

The bands CO_3^{2-} are observed at 873, 1420 and 1500 cm^{-1}. They show that they have undergone a small lag after treatment of the rats with IMI according to the results summarized in Table 3. To understand these perturbations at the bone surface, after IMI treatment, we study the stereochemistry of IMI. The spatial representation of IMI is shown schematically in Figure 4. The FTIR spectra of Confidor are shown in Figure 3. Structurally, the IMI can readily carry out a chemical bond between its active center which is represented by the chloride atom and the OH atoms on the axial axis (A6). According to the amount of IMI adsorbed on the bone, one can have an alternation on the sen-sary axis between the ions OH$^-$ and Cl$^-$ according to the following: Cl-OH-Cl-OH-Cl-OH.

The effect of UU on the bone treated with IMI is positive according to the results of X-ray diffraction and FTIR spectroscopy. Indeed, the diffractograms of (IMI+UU)-treated bones show peaks which return to their positions in 2Ө to those relating to the compound of the control group. This proves that there is a release of the pesticide (IMI) from the bone to the external environment after its action with the UU.

The spectroscopic (FTIR) results have brought us to the same conclusion, through the displacements of the bands of the groups -CH_2, PO_4^{3-} and CO_3^{2-}, while returning in their wavelength to their initial positions (control bone).

LC–MS/MS analysis

Figure 5 reports the chromatographic profiles registered at 200 and 700 nm of the UU EtOH extract. It refers to the phenolic composition (Figure 5 and Table 4).

For the reaction mechanisms of interactions between the molecules of IMI and UU, we study the stereochemical composition of UU. The EtOH extract of the aerial part of UU was analyzed by LC-MS / MS and the chromatographic profiles registered at 200 and

**Table 1.** Bone levels of calcium and phosphorus.

Groups	Calcium (mg/L)	Phosphorus (mg/L)
Control	21.225 ± 1.44	1.956 ± 1.44
50 mg/kg IMI	17.603 ± 1.34$^{\alpha**}$	1.565 ± 1.18$^{\alpha***}$
300 mg/kg IMI	16.489 ± 1.32$^{\alpha**, \beta*}$	0.891 ± 0. 23$^{\alpha***, \beta**}$
100 mg/kg UU	22.382 ± 1.34$^{\alpha*}$	2.239 ± 1.88$^{\alpha*}$
50 mg/kg IMI+100 mg/kg UU	18.311 ± 1.12$^{\beta*}$	1.869 ± 0.92$^{\beta*}$
300 mg/kg IMI+100 mg/kg UU	17.689 ± 1.32$^{£*}$	0.923 ± 0.21$^{£*}$

IMI: imidacloprid
UU: *Urtica urens* L.
Values are means ± SEM for eight rats in each group. *$p<0.05$, **$p<0.01$ and ***$p<0.001$
α: compared to controls; β: compared to 50 mg/kg of IMI; £:compared to 300 mg/kg of IMI.
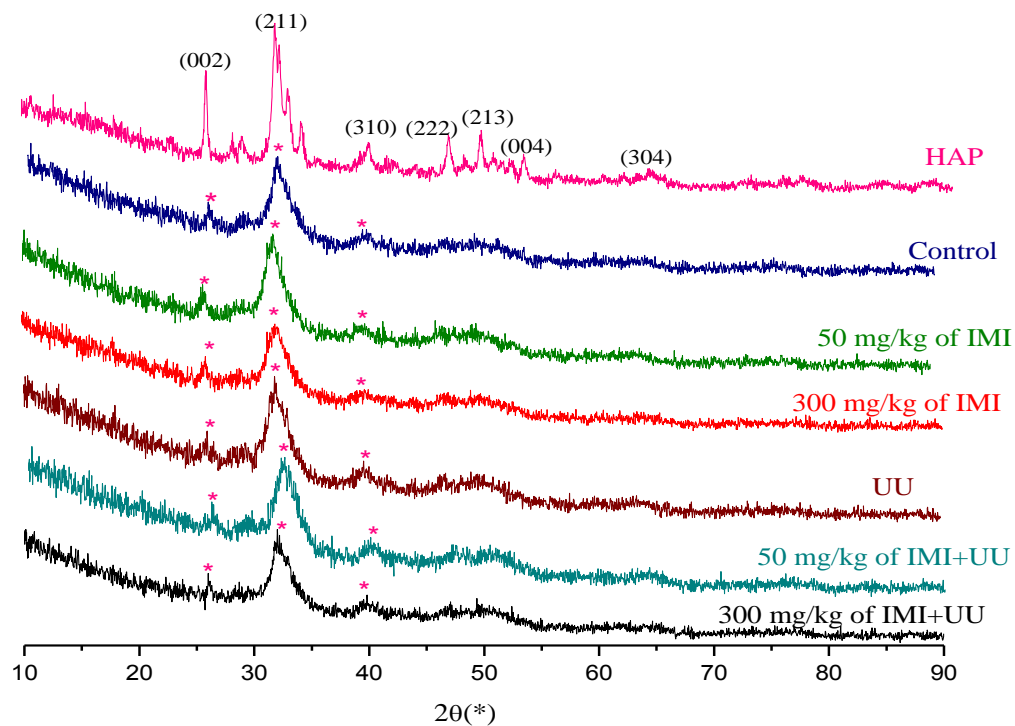
Figure 1. X-ray diffractograms of control and treated rats.

Table 2. XRD in different groups of rats.

Groups	XRD		
Peaks	(002)	(211)	(310)
HAP	27	33	41
Control	27	33	41
50 mg/kg IMI	26	32	40
300 mg/kg IMI	26	32	40
100 mg/kg UU	27	33	41
50 mg/kg IMI+100 mg/kg UU	27	33	41
300 mg/kg IMI+100 mg/kg UU	26	32	40

HAP: Hydroxyapatite
IMI: Imidacloprid
UU: *Urtica urens* L.
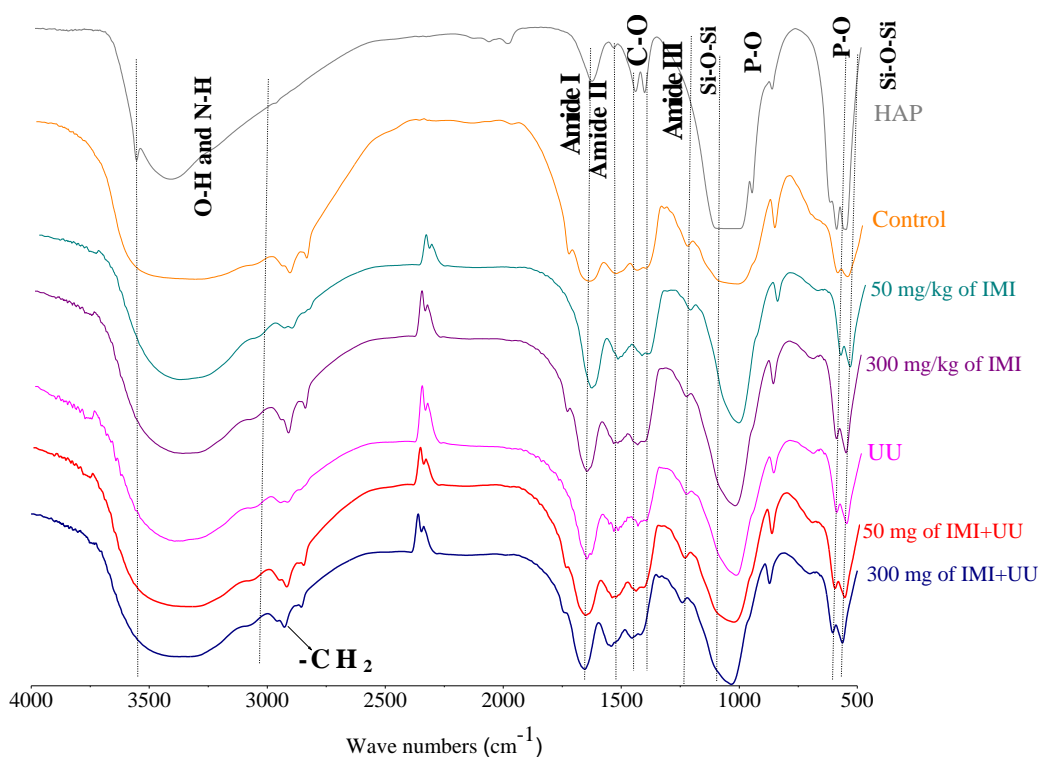
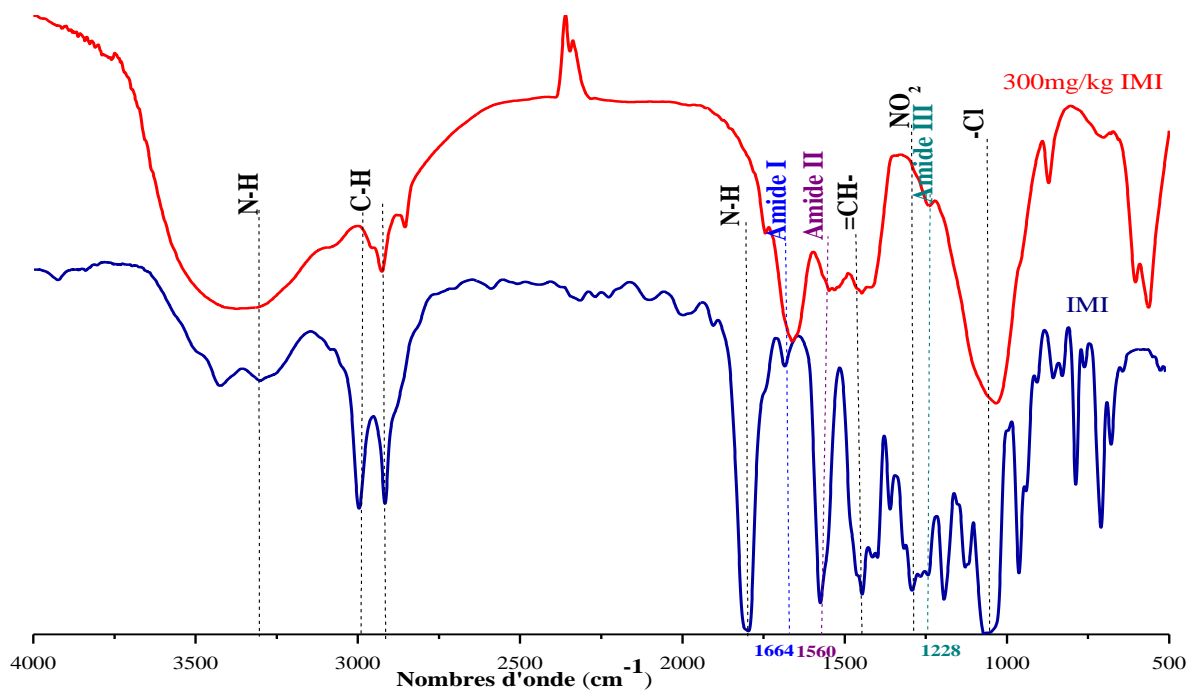**Figure. 2.** FTIR spectra of control and treated rats.

Figure. 3. FTIR analysis of IMI and femur treated with 300 mg/kg IMI.

700 nm is reported at Figure 5. The identification of the major phenolic compounds was carried out by the interpretation of the fragments found on the mass spectrum and by comparison with the literature. Table 4

Table 3. Band movements in different groups of rats.

Groups	FTIR (cm^{-1})											
	-CH$_2$				PO$_4$					CO$_3$		
HAP	-	-	-	-	1000	975	600	650	450	1500	1420	870
Control	2900	1380	665	1050	1000	950	600	650	450	1500	1420	870
50 mg/kg IMI	2900	1380	670	-	950	950	550	600	450	1450	1415	870
300 mg/kg IMI	2900	1400	670	-	950	950	550	600	450	1400	1415	865
100 mg/kg UU	2900	1380	665	1050	1000	970	550	600	450	1500	1420	870
50 mg/kg IMI + 100 mg/kg UU	2900	1380	665	1050	1000	970	550	600	450	1500	1420	870
300 mg/kg IMI + 100 mg/kg UU	2900	1400	665	1050	950	970	550	600	450	1400	1420	870

HAP: Hydroxyapatite
IMI: Imidacloprid
UU: *Urtica urens* L.
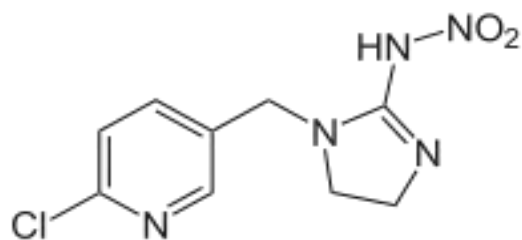
Figure. 4. Chemical formula of imidacloprid (IMI).

shows the retention times (Rt), maximum UV absorption wavelengths, mass peaks, major fragments and relative percentages of each compound.

In the reaction mechanism, the point in common between all molecules (developed formulas) is the existence of OH groups. This will react on the treated bone and exactly with the Cl$^-$ ions introduced on the senial axis through the IMI. There will be a new substitution between Cl$^-$ (treated bone) and OH$^-$ (UU) while providing a structure whose tunnels contain only OH$^-$ (control bone) and the UU contains both of OH$^-$ than of Cl$^-$, then a giant molecule is obtained between IMI and UU which is released from the bone.

Scanning electron microscopy

The results of the SEM analysis were excised at different magnifications, in Figures 6, 7, 8 and 9. The SEM results of Figures 6, 7 and 8 did not reveal the phenomenon of alteration of IMI-treated bone. However, with a grossissement of 1 µm (Figure 9), we can clearly see the phenomenon of textural alteration in the IMI-treated bones (B, C). UU injection shows architecture within the bone resembling that of the control bone.

Bone study microanalysis-energy spectrometry (EDX)

Microanalysis - energy spectroscopy (EDX) is used to obtain the distribution mapping of the different elements by X-ray backscattering. The results obtained for the control group, treated group with 50 mg/kg IMI, treated group with 300 mg/kg IMI, treated group with 100 mg/kg UU, treated group with 50 mg/kg IMI+100 mg/kg UU, and treated group with 300 mg/kg IMI+100 mg/kg UU are shown in Figure 10 A, B, C, D, E and F, respectively.

The composition of femurs of different groups was quantified by measuring the concentration of phosphate and calcium. The quantitative analyzes (atomic%) by EDX of the elements in the different groups were presented in Table 5.

The results show that the Ca/P ratio is 1.8 (normal between 1.7 and 2) in control femurs and (UU+IMI)-treated femurs. However, this ratio decreases to 1.5 in IMI-treated femurs. Generally, the reduction of this ratio to above 1.67 (Bonel et al., 1988) is due to a structural and microstructural disturbance of the bone, under the action of several phenomena. In our study, that we noted the decrease of this ratio. This ratio increases again to reach the value 1.8 following the addition of UU. This technique confirmed our previous results (obtained through FTIR, XRD, etc), which showed the protective effect of UU against the toxic or disruptive effect of IMI.

DISCUSSION

We aimed to evaluate the effect of IMI on bone remodeling and the protective effect of UU EtOH extract using physico-chemical techniques (FTIR, XRD, SEM) and analytical methods (Ca and P).
Analytical analyzes of Ca and P levels in bone showed a decrease in their levels in IMI-treated groups. Our results showed also an increase of these levels in (IMI+UU)-treated group. We noted an increase of Ca and P, in the (IMI+UU)-treated groups as compared to the IMI-treated groups. Qualitatively, UU has a positive effect on phospho-calcium disorder, but on the quantitative level this effect remains to be checked if the dose of UU is increased. These results are reinforced by those obtained
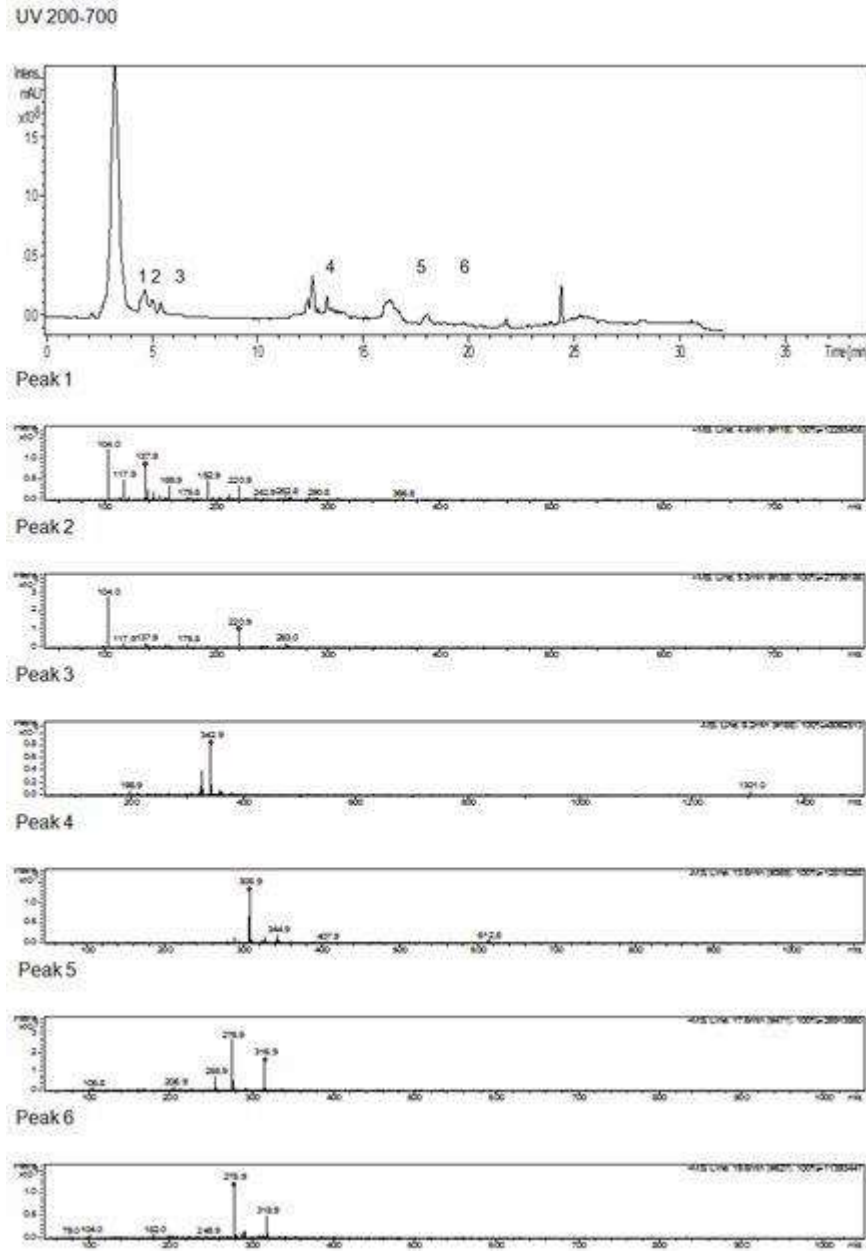
Figure 5. LC/MS chromatogram of the UU ethanol extract at two different wavelengths (200 and 700 nm).
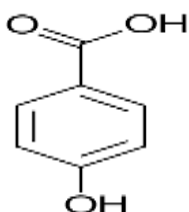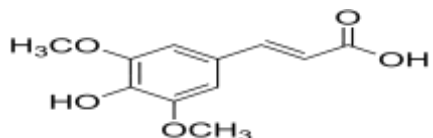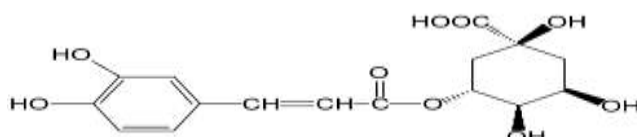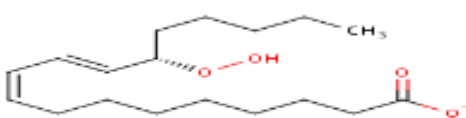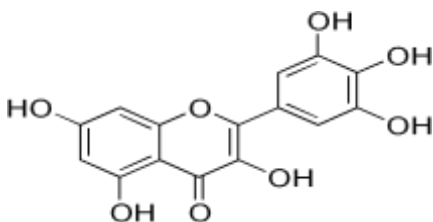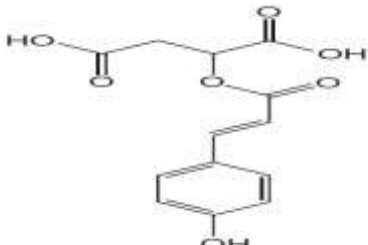
by EDX analysis, which showed a Ca/P ratio of 1.8 for control group and decreased to 1.5 for IMI-treated groups. Our experimental results show that IMI modifies the mineral composition of the femurs and disrupts the phospho-calcium balance. Mackay (1953) showed that the presence of HPO_4 hydrogenophosphate, which justifies the value of its low Ca/P ratio with respect to the stoichiometric value of 1.67, leads to structural disorder of the apatitic matrix. According to Raynaud et al. (2002), the modification of the Ca/P ratio causes structural and textural variations of the powder studied.

Several studies (Bhardwaj et al., 2010; Kapoor et al.,

2011) have shown that exposure to IMI can affect different metabolic processes (calcium and phosphorus metabolism) and the organs (kidney, liver, ovary) which are directly related to bone metabolism.

In addition, X-ray diffraction (XRD) showed that there are displacements at the values of Ө. IMI increases the crystallographic parameters (a, b, c) and thus inflates the crystalline mesh of the bone (Yashima et al., 2003). Masmoudi et al. (2006) showed the same results of expansion of the mesh in a synthetic bone following the introduction of melanin (cuttlefish ink granules) in an asymmetric microfiltration ceramic membrane (Active

Table 4. Spectral data acquired by the LC–MS analyses of the main antioxidants of the UU ethanol extract.

Peak number	tR (min)	UV (nm)	LC–MS analyses (m/z)	Structure	Relative percentage (%)	Developed formulas
1	4.4	200-700	137.9	p-Hydroxy benzoic acid	8.58	
2	5.3	200-700	220.9	Sinapic acid	13.75	
3	6.2	200-700	342.9	Chlorogenic acid	21.34	
4	13.6	200-700	308.9	Japonic acid	19.22	
5	17.6	200-700	316.9	Myricetin	19.72	
6	19.6	200-700	278.9	p-Coumaroyl malate	17.36	

layers) based on synthesized lacunar hydroxyapatite (HAP).

Also, Hamdi et al. (2007) have shown in their previous work during the synthesis of a series of bismuth and sodium-based apatite based on bismuth and sodium, an example of the formula: $Pb_{5,78}Bi_{0,81}Ca_{0.60}Na_{2.81}(PO_4)6$. These compounds are of apatite structure crystallizing in the hexagonal system of P63/m space group. In this work, the X-ray diffraction showed, following the substitution of calcium by bismuth and lead, for an increase in the volume of the bone mesh. This has been explained by the fact that the ionic rays of the two substitutes (Bi, Pb) are greater than that of the substituted element (Ca).

The infrared absorption spectroscopy (FTIR) analyzes show that there are displacements in the number of waves of the $-CH_2$, PO_4^{3-} and CO_3^{2-} in IMI6 treated groups. This confirms even more the disruptive effect of
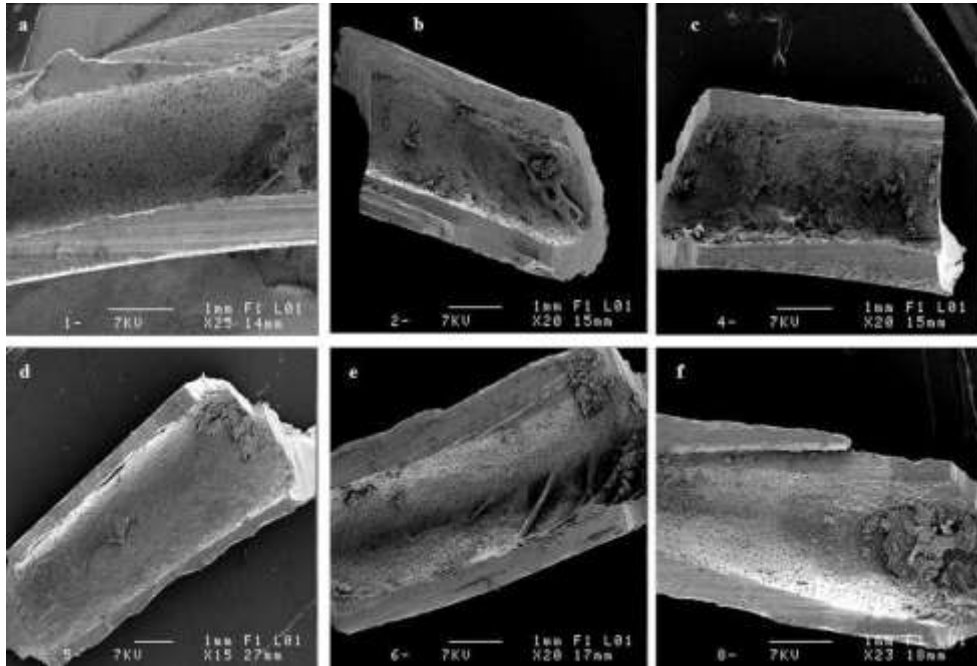
Figure 6. General appearance of the diaphysis of treated rats with IMI, IMI+UU or UU for 60 days. (a) Femur section of control rats; (b) Femur section of treated rats with 50 mg/kg IMI; (c) Femur section of treated rats with 300 mg/kg IMI; (d) Femur section of treated rats with 100 mg/kg UU; (e) Femur section of treated rats with 50 mg/kg IMI+100 mg/kg UU; (f) Femur section of treated rats with 300 mg/kg IMI+100 mg/kg UU.
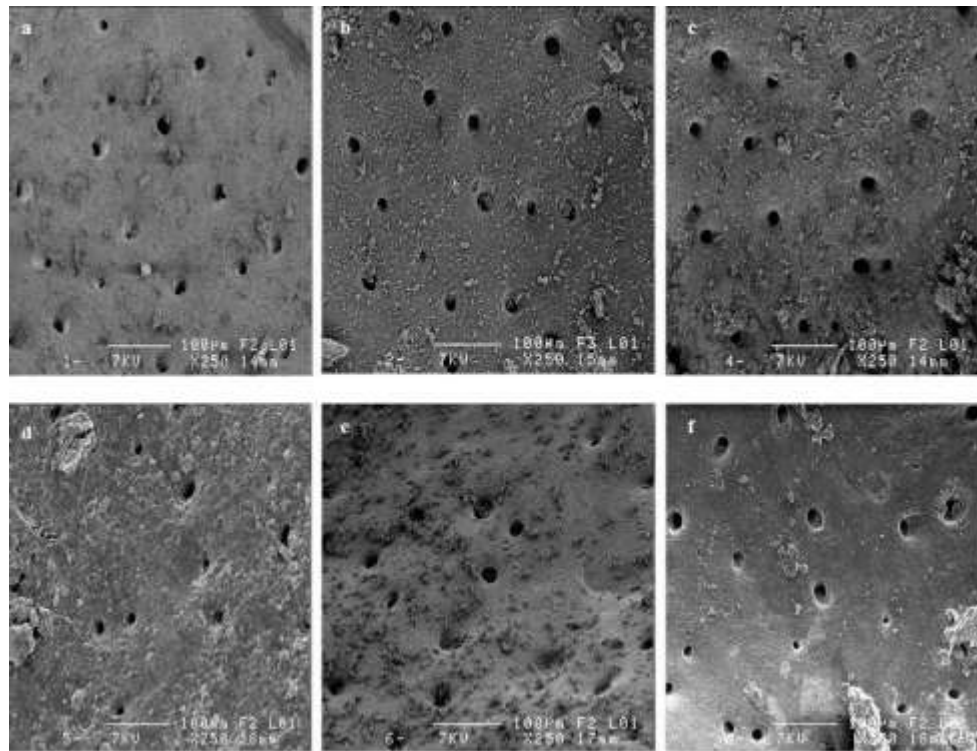

Figure 7. Appearance of endosteum of treated rats with IMI, IMI+UU or UU for 60 days. (a) Femur section of control rats; (b) Femur section of treated rats with 50 mg/kg IMI; (c) Femur section of treated rats with 300 mg/kg IMI; (d) Femur section of treated rats with 100 mg/kg UU; (e) Femur section of treated rats with 50 mg/kg IMI+100 mg/kg UU; (f) Femur section of treated rats with 300 mg/kg IMI+100 mg/kg UU.
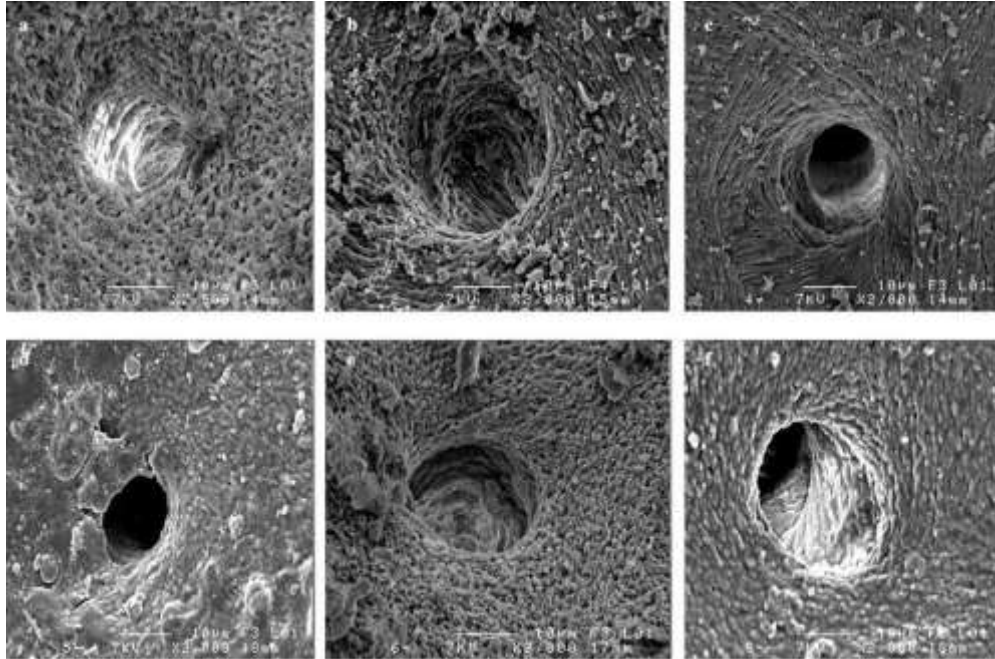
Figure. 8. Apparence of the cancellous bone of treated rats with IMI, IMI+UU or UU for 60 days. (a) Femur section of control rats; (b) Femur section of treated rats with 50 mg/kg IMI; (c) Femur section of treated rats with 300 mg/kg IMI; (d) Femur section of treated rats with 100 mg/kg UU; (e) Femur section of treated rats with 50 mg/kg IMI+100 mg/kg UU; (f) Femur section of treated rats with 300 mg/kg IMI+100 mg/kg UU.
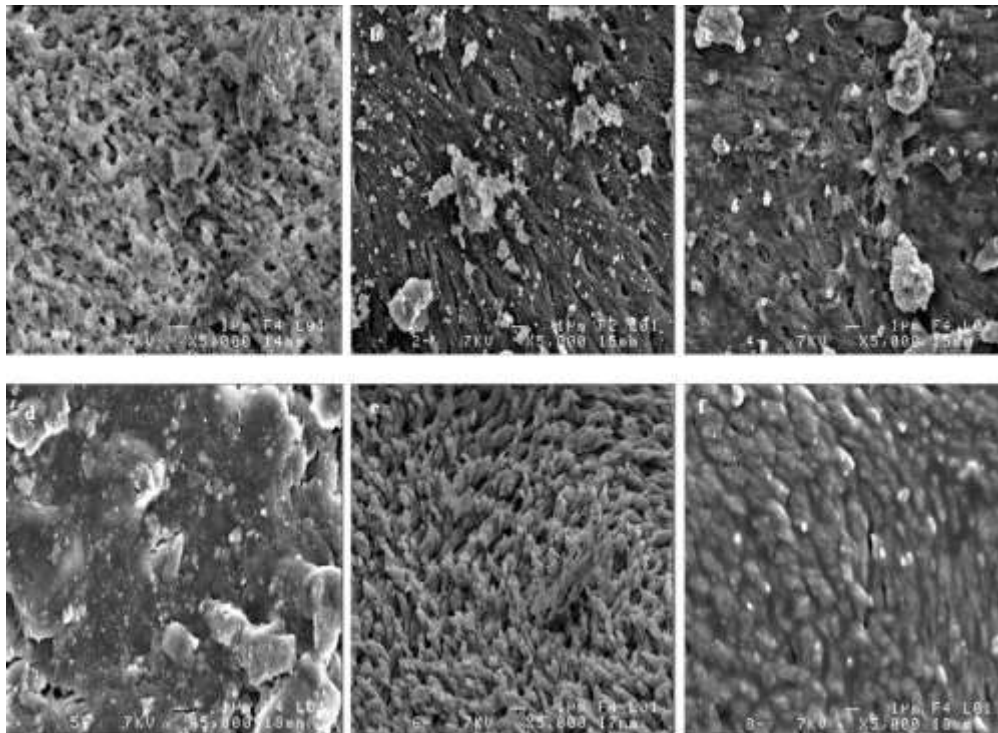

Figure. 9. Scanning electron microscopy observation of compact bone. (a) Femur section of control rats; (b) Femur section of treated rats with 50 mg/kg IMI; (c) Femur section of treated rats with 300 mg/kg IMI; (d) Femur section of treated rats with 100 mg/kg UU; (e) Femur section of treated rats with 50 mg/kg IMI+100 mg/kg UU; (f) Femur section of treated rats with 300 mg/kg IMI+100 mg/kg UU.
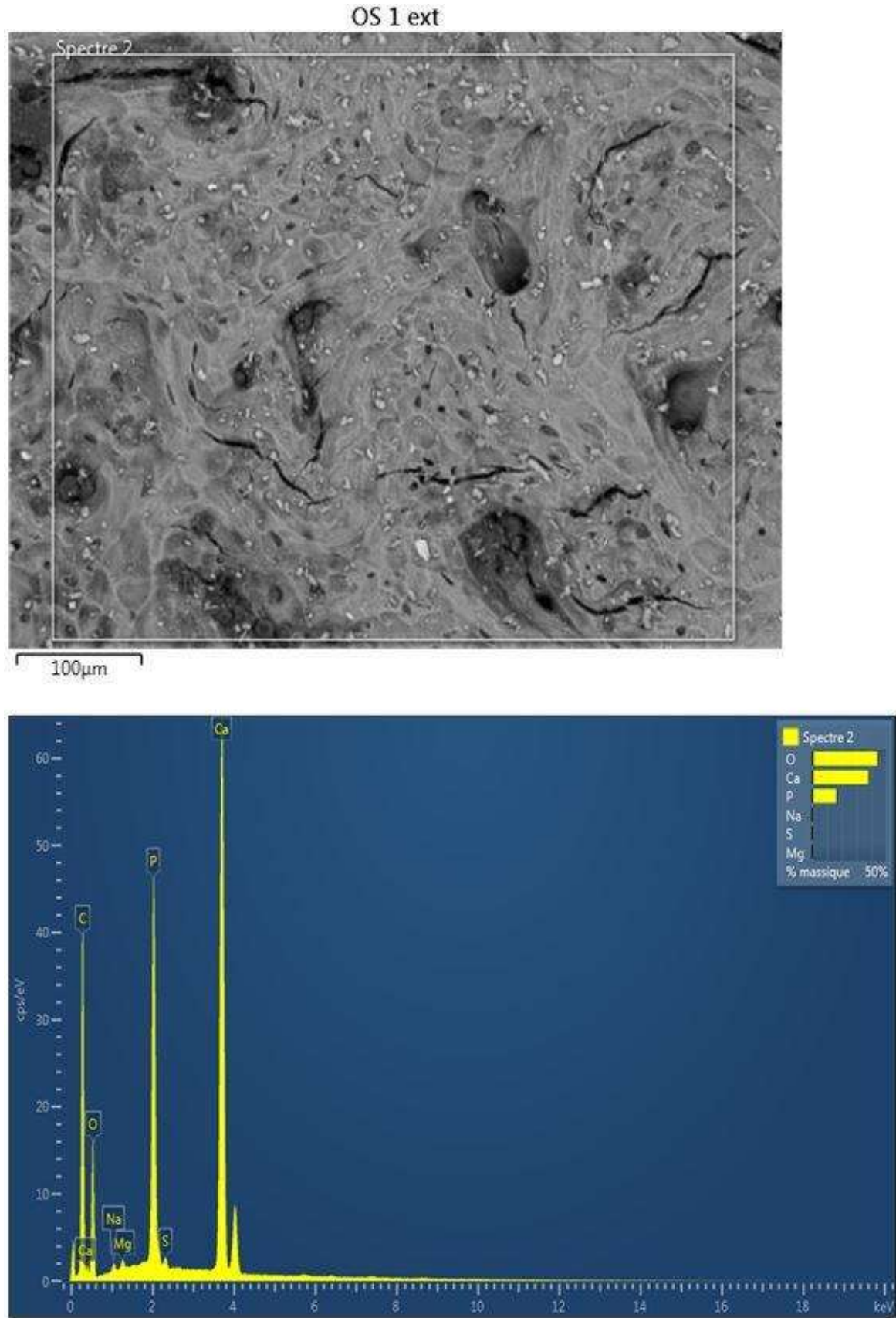
Figure 10A. EDX spectrum and maps distributions of femoral components of control rats after 60 days.
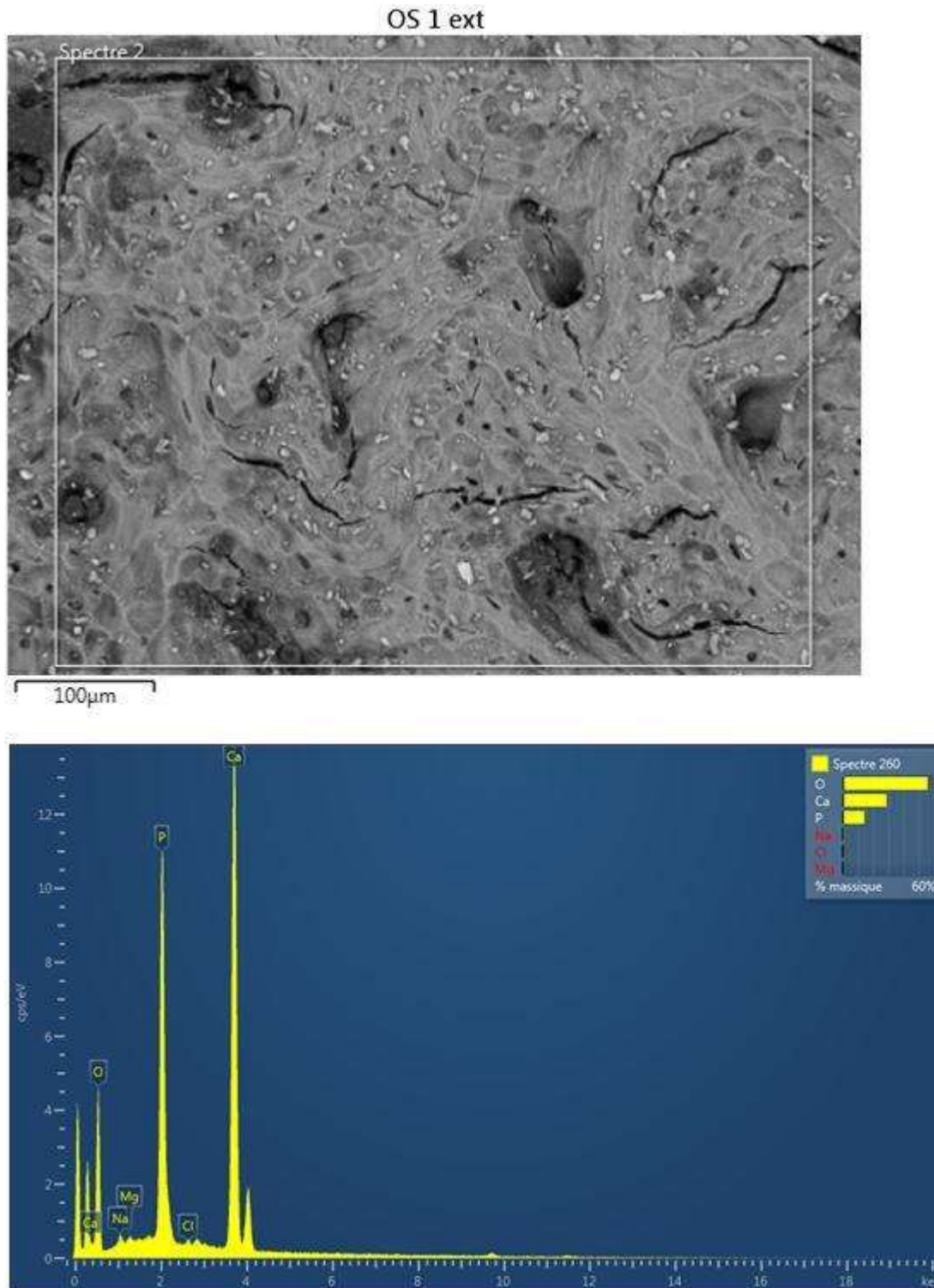
Figure 10B. EDX spectrum and maps distributions of femoral components of treated rats with 50 mg/kg of IMI.

IMI on the bone remodeling through the attachment of this molecule with the molecules of the bone. Hammami et al. (2015) have studied the physico-chemical interaction between the nucleotide adenosine monophosphate (AMP) and the synthetic biomimetic apatite. FTIR spectroscopic analyzes confirmed this chemical interaction between AMP molecules and the surface of apatite nanocrystals.
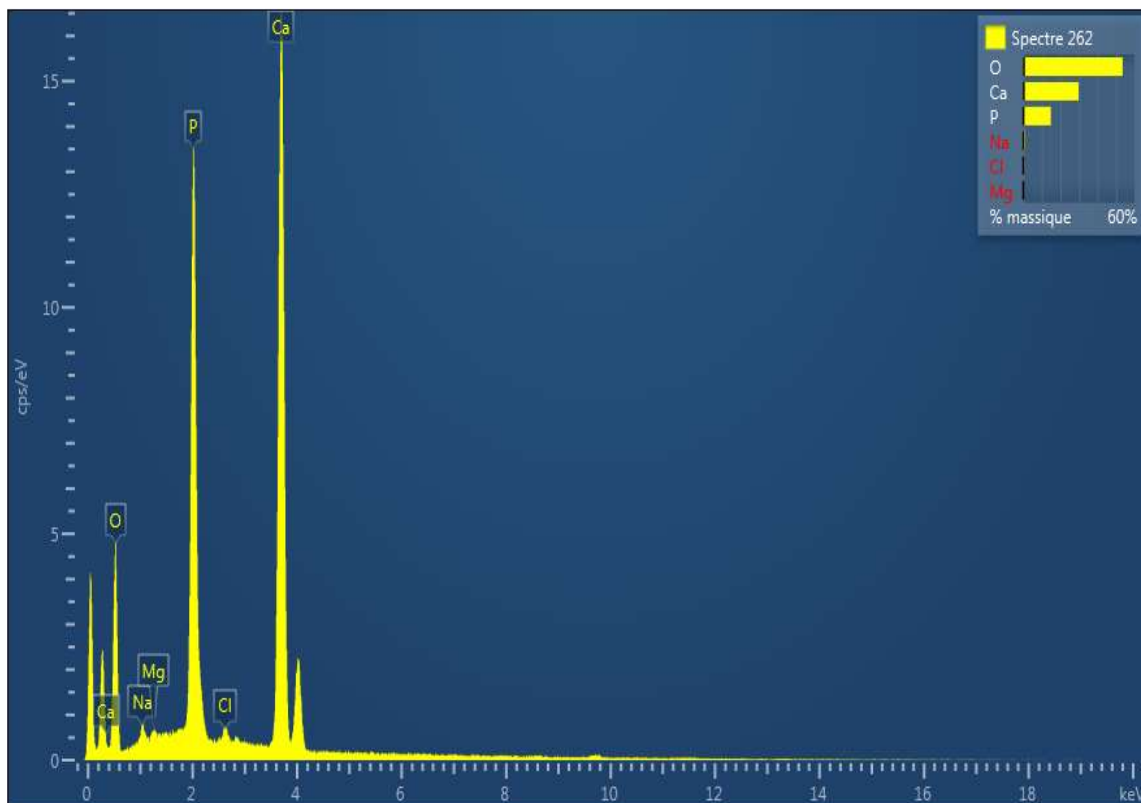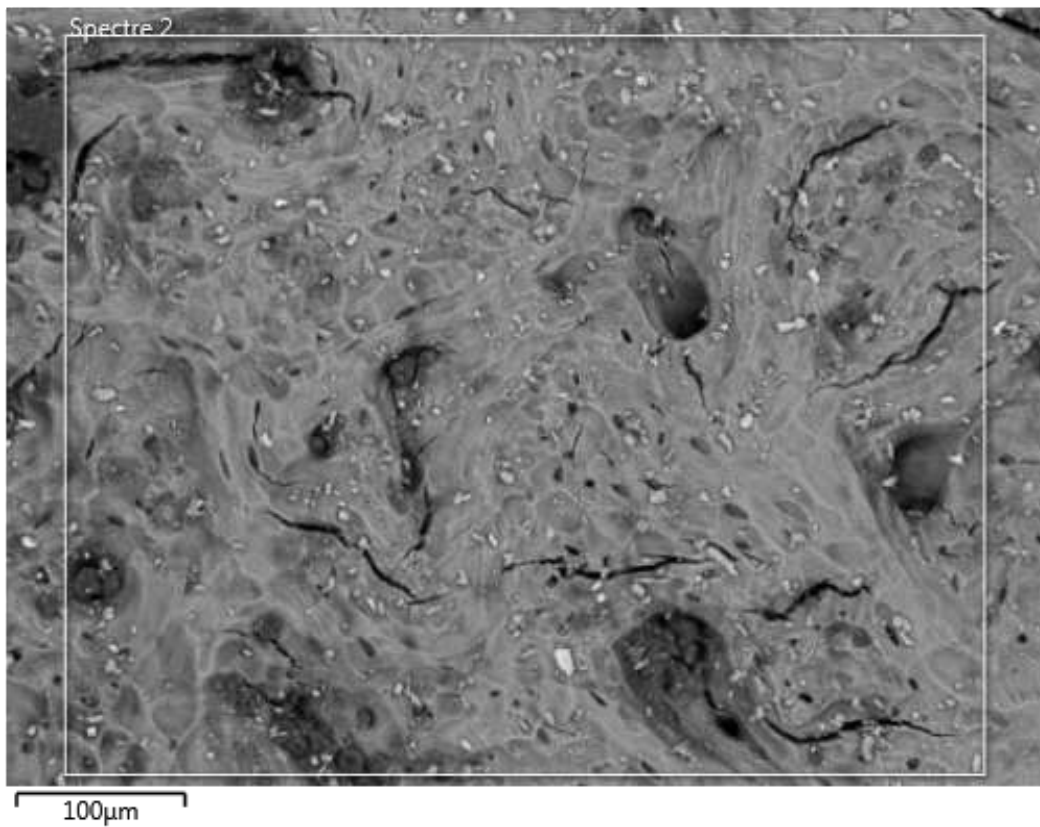
Figure 10C. EDX spectrum and maps distributions of femoral components of treated rats with 300 mg/kg of IMI.

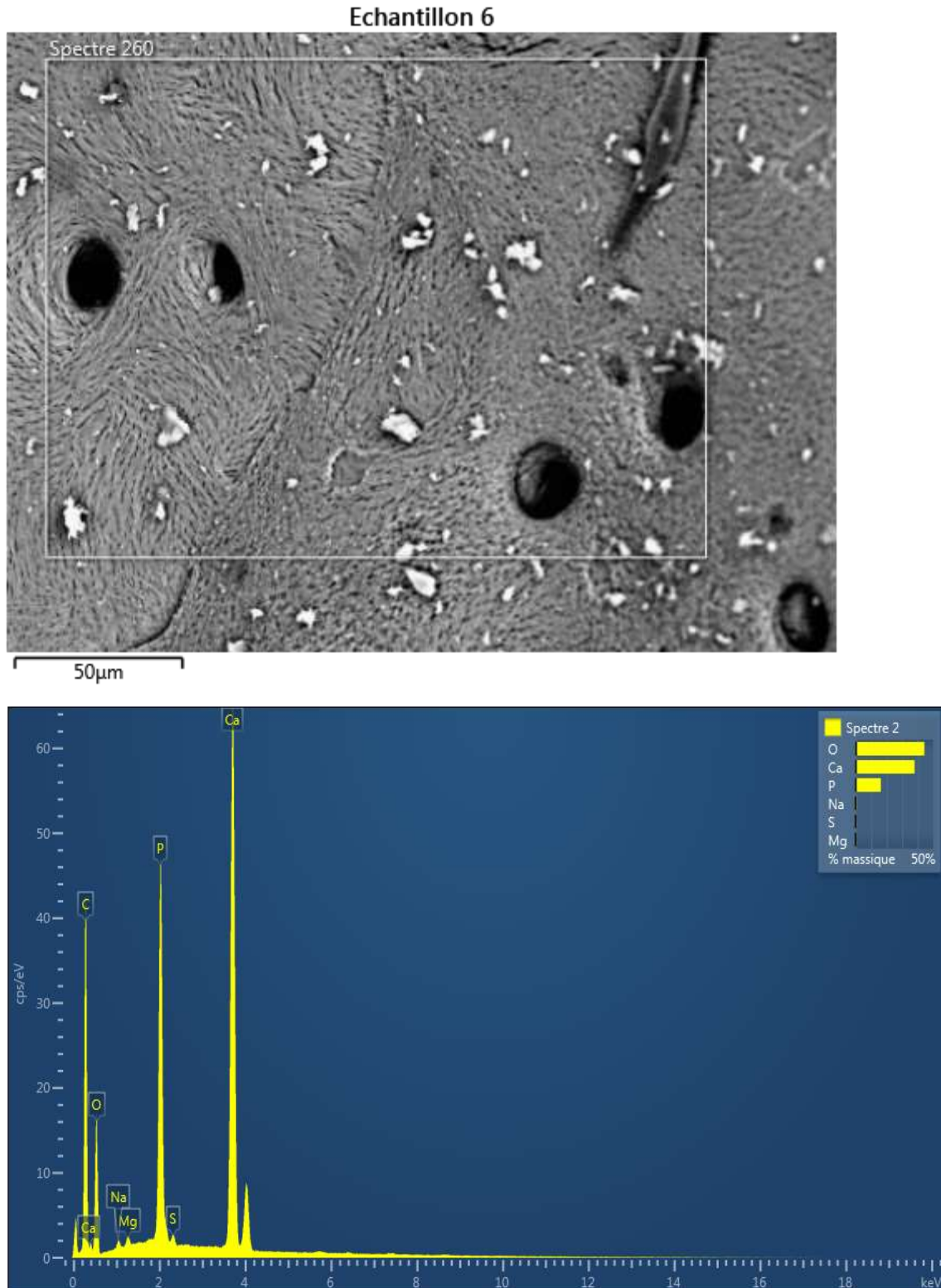**Figure 10D.** EDX spectrum and maps distributions of femoral components of treated rats with UU for 60 days.

Similarly, Hammami et al. (2014) have also studied the association of adenosine 5'-triphosphate (ATP) molecules and fine hydroxyapatite (HAP). They have evaluated the effects of the presence of ATP molecules, while using physico-chemical techniques, within the apatitic surface. The hybrids were produced by combining increasing
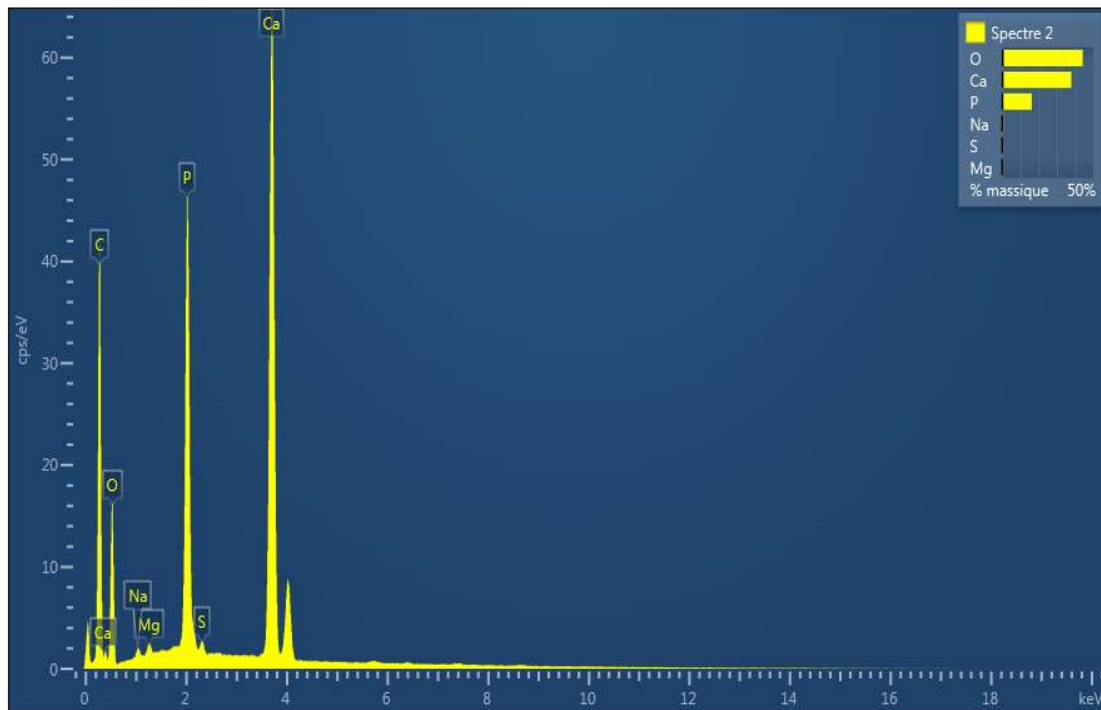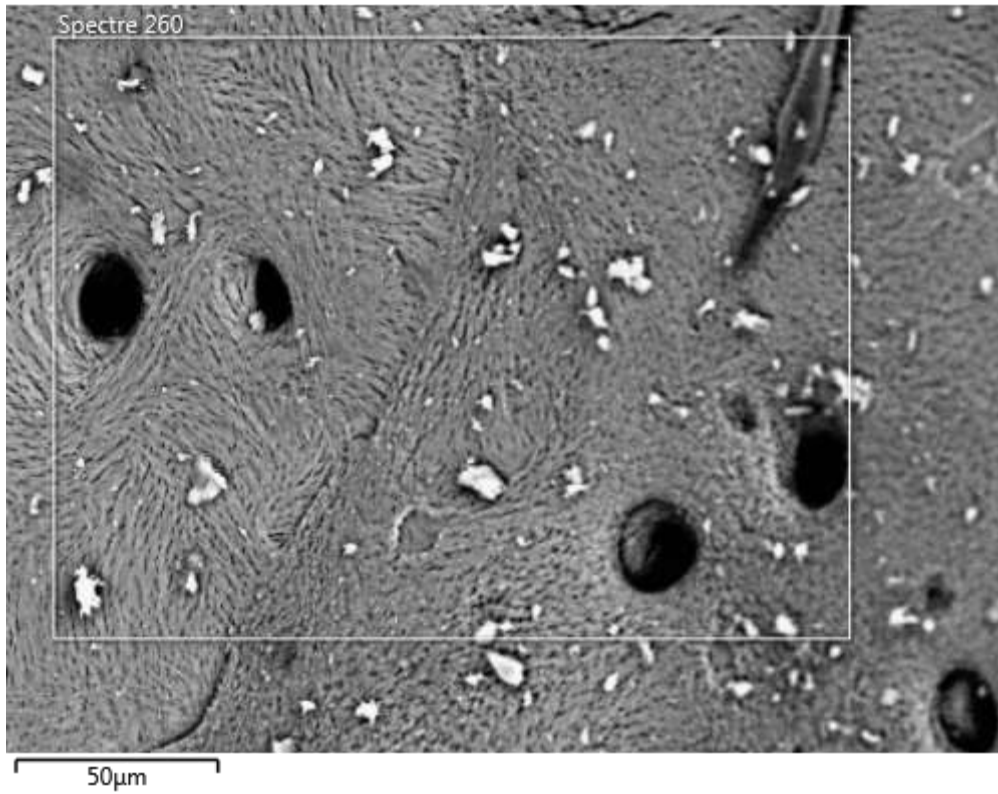
Figure 10E. EDX spectrum and maps distributions of femoral components of treated rats with 50 mg/kg of IMI+UU.

amounts of ATP disodium hydrate salt with hydroxyapatite, resulting in so-called "organoapatites".

The structure and the composition of the polycrystalline hybrid compounds obtained have been studied by

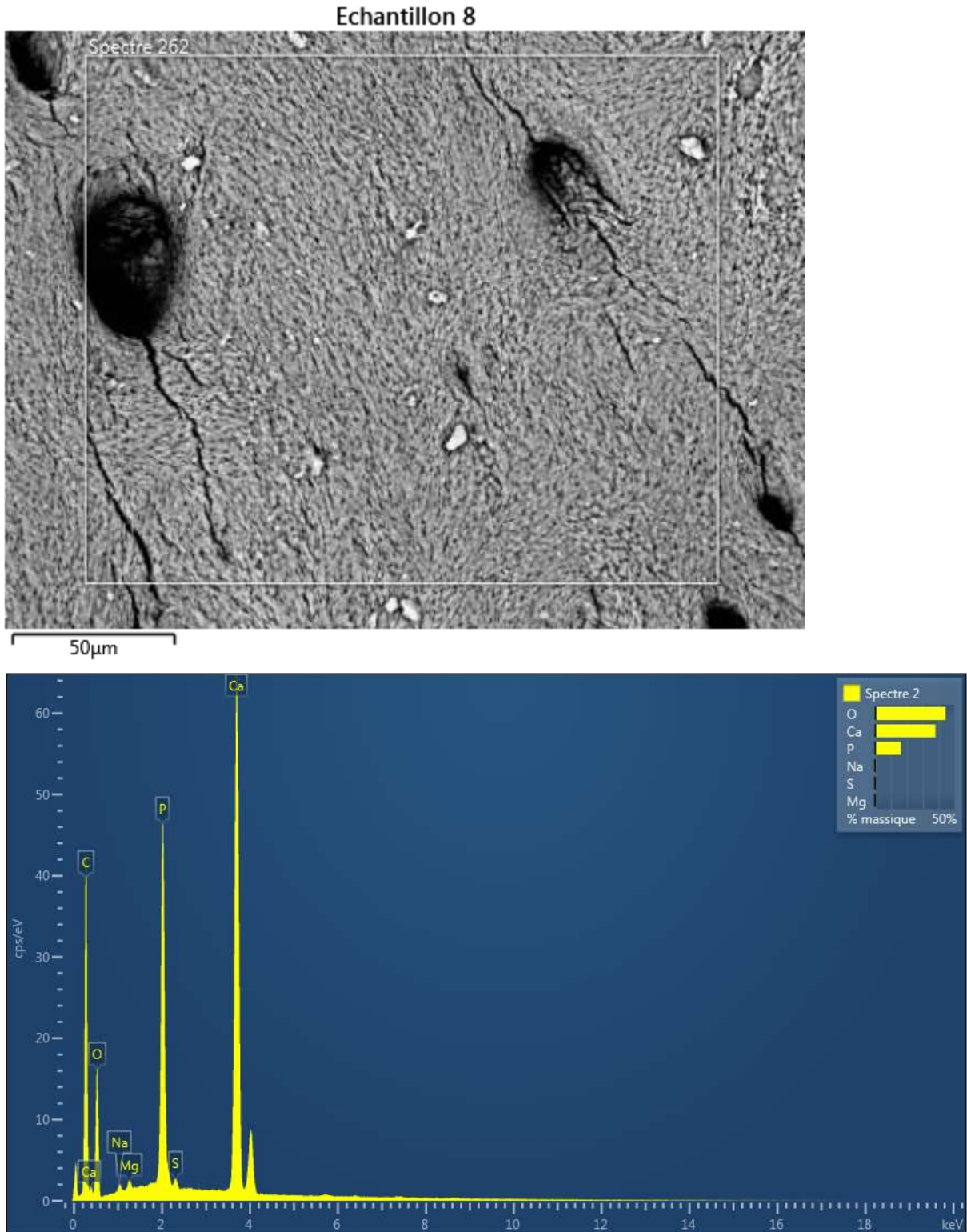**Figure 10F.** EDX spectrum and maps distributions of femoral components of treated rats with 300 mg/kg of IMI+UU.

techniques such as FTIR. The decrease in the intensity of the bands is due to the increase in the amount of ATP attached to the bone structure.

This confirms our results obtained through the use of DRX and FTIR techniques, which showed that IMI disturbs bone remodeling in rats.

Table 5. Quantitative analysis (atomic%) of elements determined from EDX in the different groups of rats.

Groups	Atomic %							
	O	Na	Mg	P	S	Cl	Ca	Ca/P
Control	64.29	0.61	0.48	12.18	0.40	-	22.04	1.80952381
50 mg/kg IMI	73.88	0.77	0.24	9.72	0.17	0.17	15.24	1.56790123
300 mg/kg IMI	72.14	0.95	0.26	10.33		0.30	16.03	1.5517909
100 mg/kg UU	64.29	0.61	0.48	12.18	0.40	-	22.04	1.80952381
50 mg/kg IMI + 100 mg/kg UU	64.29	0.61	0.48	12.18	0.40	-	22.04	1.80952381
300 mg/kg IMI + 100 mg/kg UU	64.29	0.61	0.48	12.18	0.40	-	22.04	1.80952381

IMI: Imidacloprid
UU: *Urtica urens* L.

In addition, we have demonstrated with SEM analysis a phenomenon of textural alteration in the bone treated by different doses of IMI and which increases with the dose. It could be explained by a disturbance of bone remodeling, with delayed ossification and confirms that IMI disturbs well the bone remodeling. Similarly, Badraoui et al. (2007a) showed that tetradifon (pesticide estrogen-like) disrupted the mineral composition of bone especially calcium and phosphorus which increased in content. However, MEB analysis did not demonstrate the structural alteration in the general organization of the femoral parts in the treated rats. This is probably due to the oestrogen-like effect of tetradifon. Indeed, estrogen inhibits remodeling and enhances bone formation. Tetradifon does not appear to have a deleterious effect on bone remodeling.

The XRD analyzes revealed a return of the peaks to their initial position for the (IMI+UU)-treated groups. UU injection with its intake of minerals (Ca and P) has no influence on the mesh for the high dose in IMI (300 mg/kg). So, calcium and phosphorus have remained either labile on the surface or that the quantity of minerals contributed by UU is insufficient to remedy the toxic effect of IMI on the bone.

The UU injection in the presence of IMI in the bone causes a release of the pesticide. The increase in the dose of IMI and always in the presence of UU shows an increase in the crystallographic parameters, which proves the existence of the pesticide in the bone. This is in agreement with the analytical results which showed that quantity of UU is insufficient to neutralize all the toxicity of IMI. FTIR results have brought us to the same conclusion, through the displacements of bands, -CH_2, PO_4^{3-} and CO_3^{2-}, while returning in their wavelength to their initial positions (control bone). UU has a protective effect against the toxicity caused by IMI. Our results were in agreement with the study of Barraza-Garza et al. (2016) who showed that analysis of FTIR spectra can provide valuable data on the protective effect of the polyphenolic compounds effect in rat enterocytes against H_2O_2-induced oxidative stress.

SEM results showed that (IMI+UU)-treated groups have normal bones compared to IMI-treated groups. This could be attributed to the presence of bioactive components in the UU EtOH extract (phenolic compounds, flavonoids, minerals (Calcium, Phosphorus, etc)), which stimulates the osteoblastic activity and thanks to the richness of these compounds in OH^-.

OH^- will react on the treated bone and exactly with Cl^- introduced on the senial axis through the IMI. There will be a new substitution between Cl^- (treated bone) and OH^- (UU) while providing a structure whose tunnels contain only OH^- (control bone) and the UU contains both of the ions OH^- than of the Cl^- ions, then a giant molecule is obtained between IMI and UU which is released from the bone. Very similar results to this study were obtained by Suwalsky et al. (2015), SEM analysis demonstrated the highly protective effect of *Hilesia magellanica* (Coicopihue) from Chilean Patagonia against oxidative damage. Suwalsky et al. (2007) also showed the protective effect of *Ugni molinae Turcz* against oxidative damage of human erythrocytes by scanning electron microscopy (SEM).

In another work, Radhakrishnan et al. (2018) investigated that *Pedalium murex Linn* extract can decreased crystal size and prevented the aggregation of calcium oxalate crystals using SEM and DRX.

Ben Amara et al. (2012) have evaluated the ability of selenium, used as a nutritional supplement, to alleviate bone deficiencies in mothers treated with methimazole, an antithyroid drug.

Treatment with methimazole reduced the length and weight of the femur in pups compared to controls. The activities of the antioxidant enzymes of the femur, superoxide dismutase, catalase and glutathione peroxidase have decreased. Lipid peroxidation showed an increase in the high rates of malondialdehyde in the femur. Methimazole also caused a significant decrease in Ca and P levels in bone. In addition, resistant tartrate acid phosphatase was increased, while total alkaline phosphatase was reduced. The administration of selenium in the diet has improved the biochemical parameters cited above. This study suggests that selenium is an important protective element that can be used as a dietary supplement protecting against bone deficiencies.

In our study, UU injection also moderated the phospho-calcium disorder caused by IMI, and has a protective effect against this phospho-calcium imbalance. UU injection provides supplements in minerals (especially Ca and P) and vitamin D which leads to improved bone formation and mineralization. These results are comparable to those obtained by Von Rosenberg et al. (2007) who demonstrated that EtOH extract of *Solanum glaucophyllum* and *Trisetum flavenscens* is capable to improve bone mineral density through vitamin D.

Indeed, Gargouri et al. (2016) have conducted a study of the toxicity of lead in bone development in pups as well as the protective role Spirulina (*Arthrospira platensis*) added to the diet. In fact, they showed that there was a decrease in the weight and length of the femur, as well as a decrease in calcium and phosphorus in the bones with the accumulation of lead. Lipid peroxidation was increased, while the activities of superoxide dismutase, catalase, and glutathione peroxidase in the femur decreased. Bone disorders were confirmed by histological changes in the femur. However, no damage or biochemical changes were observed in pups fed Spirulina and lead. These results strongly suggest that consumption of this plant alleviate all previous parameters to near-normal levels. Spirulina therefore plays a very important protective role in rats by inhibiting the toxicity induced by lead due to its richness of bioactive compounds.

CONCLUSION

Our study indicated that the toxicity of imidacloprid has affected bone mineralization of female rats. It is suggested that protective effects of UU are due to its antioxidant activity. UU injection can attenuate the phosphocalcic disorder caused by imidacloprid and has a protective effect against the modification of the phosphocalcium balance. According to these findings, further studies are suggested to evaluate the effects *Urtica urens* extracts as therapeutic agents in osteoporosis.

REFERENCES

Álvarez-Lloret P, Rodríguez-Navarro AB, Romanek CS, Ferrandis P, Martínez-Haro M, Mateo R, **2014**. Effects of lead shot ingestion on bone mineralization in a population of red-legged partridge (*Alectoris rufa*). Sci Total Environ, 1: 34-39.

Badraoui R, Abdelmoula NB, Sahnoun Z, Fakhfakh Z, Rebai T, **2007a**. Effect of subchronic exposure to tetradifon on bone remodelling and metabolism in female rat. C. R. Biol, 330: 897-904.

Barraza-Garza G, Castillo-Michel H, de la Rosa LA, Martinez-Martinez A, Pérez-León JA, Cotte M, Alvarez-Parrilla E, **2016**. Infrared Spectroscopy as a Tool to Study the Antioxidant Activity of Polyphenolic Compounds in Isolated Rat Enterocytes. Oxid Med Cell Longev, 9245150.

Baxley MN, Hood RD, Vedel GC, Harrison WP, Szczech GM, **1981**. Prenatal toxicity of orally administered sodium arsenite in mice. Bull Environ Contam Toxicol, 26: 749-756.

Ben Amara I, Troudi A, Soudani N, Guermazi F, Zeghal N, **2012**. Toxicity of methimazole on femoral bone in suckling rats: alleviation by selenium. Exp Toxicol Pathol, 64: 187-95.

Bhardwaj S, Srivastava MK, Kapoor U, Srivastava LP, **2010**. A 90 days oral toxicity of imidacloprid in female rats: Morphological, biochemical and histopathological evaluations. Food Chem Toxicol, 48: 1185-1190.

Bonel G, Heughebaert JC, Heughebaert M, Lacout JL, Lebugle A, **1988**. Apatitic calcium orthophosphates and related compounds for biomaterials preparation. Ann NY Acad Sci, 523: 115-130.

Boskey A, **Mendelsohn** R, **2005**. Infrared analysis of bone in health and disease. J Biomed Opt, 10: 031102.

Boskey AL, Di Carlo EF, Gilder H, Donnelly R, Weintroub S, **1988**. The effect of short-term treatment with vitamin D metabolites on bone lipid and mineral composition in healing vitamin D-deficient rats. Bone, 9: 309-318.

Boskey AL, **Marks** SCJr, **1985**. Mineral and matrix alterations in the bones of incisors-absent (ia/ia) osteopetrotic rats. Calcif Tissue Int, 37: 287-92.

Boskey AL, Pleshko N, Doty SB, Mendelsohn R, **1992**. Applications of Fourier-transform infrared (FT-IR) microscopy to the study of mineralization in bone and cartilage. Cells Mater, 2: 209-220.

Bouafou KGM, Kouamé KG, Offoumou AM, **2007**. Bilan azoté chez le rat en croissance de la farine d'asticots séchés. Tropicultura, 25: 70-74.

Camacho NP, Hou L, Toledano TR, Ilg WA, Brayton CF, Raggio CL, Root L, Boskey AL, **1999**. The material basis for reduced mechanical properties in oim mice bones. J Bone Miner Res, 14: 264-72.

Casida JE, **Durkin** KA, **2013**. Neuroactive insecticides: targets, selectivity, resistance, and secondary effects. Annu Rev Entomol, 58: 99-117.

Doukkali Z, Taghzouti K, Bouidida EL, Nadjmouddine M, Cherrah Y, Alaoui K, **2015**. Evaluation of anxiolytic activity of methanolic extract of *Urtica urens* in a mice model. Behav. Brain Funct, 11: 19.

Duzguner V, **Erdogan** S, **2010**. Acute oxidant and inflammatory effects of imidacloprid on the mammalian central nervous system and liver in rats. Pestic Biochem Phys, 97: 13-18.

Eiben R, **Kaliner** G, **1991**. NTN 33893 (Imidacloprid): Chronic Toxicity and Carcinogenicity Studies on Wistar Rats. (Administration in Food Over 24 Months): Lab Project Number: 19925: 100652. Prepared by Bayer AG. Departement of Toxicology. 1323 p.; MRID 42256331.

Eiben R, **Rinke** M, **1989**. Subchronic Toxicity on Wistar Rats. Administration in the Feed for 96 Days. Prepared by Bayer AG. Department of Toxicology. Fachbereich Toxikologie Wuppertal, Germany. Study No. 100036; DPR;Vol. 51950-0005 # 119467.

Emam H, Ahmed E, Abdel-Daim M, **2018**. Antioxidant capacity of omega-3-fatty acids and vitamin E against imidacloprid-induced hepatotoxicity in Japanese quails. Environ Sci Pollut Res, 25: 11694-11702.

Gargouri M, Saad HB, Magne C, El Feki A, **2016**. Toxicity of lead on femoral bone in suckling rats: Alleviation by Spirulina. Res Rev Biol Sci, 11: 3.

Gee A, **Dietz** VR, **1953**. Determination of phosphate by differential spectrophotometry. Ann Chem, 25: 1320–1324.

Glimcher MJ, **1998**. The nature of the mineral phase in bone: Biological and clinical implications. In Metabolic Bone Disease and Clinically Related Disorders; Alvioli LV, Krane, SM, Eds.; Academic Press: San Diego, CA, pp 23-50.

Hamdi B, El Feki H, Savariault JM, Salah AB, **2007**. Synthesis and distribution of cations in substituted lead phosphate lacunar apatites. Mater Res Bull, 42: 299-311.

Hammami K, El Feki H, Marsan O, Drouet C, **2015**. Adsorption of nucleotides on biomimetic apatite: the case of adenosine 5′ monophosphate (AMP). Appl Surf Sci, 353: 165-172.

Hammami K, Elloumi J, Aifa S, Drouet C, El Feki H, **2014**. Synthesis and characterization of hydroxyapatite ceramics organofunctionalized with ATP (adenosine triphosphate). J. Adv. Chem, 9: 1787-1797.

Jeschke P, Nauen R, Schindler M, Elbert A, **2010**. Overview of the status and global strategy for neonicotinoids. J Agr Food Chem, 59: 2897-2908.

Kapoor U, Srivastava MK, Srivastava LP, **2011**. Toxicological impact of

technical imidacloprid on ovarian morphology, hormones and antioxidant enzymes in female rats. Food Chem Toxicol, 49: 3086-3089.

Li D, Ge X, Liu Z, Huang L, Zhou Y, Liu P, Qin L, Lin S, Liu C, Hou Q, Li L, Cheng H, Ou S, Wei F, Shen Y, Zou Y, Yang X, **2019**. Association between long-term occupational manganese exposure and bone quality among retired workers. Environ Sci Pollut Res Int, 3.

Lv Y, Bing Q, Lv Z, Xue J, Li S, Han B, Yang Q, Wang X, Zhang Z, **2019**. Imidacloprid-induced liver fibrosis in quails via activation of the TGF-β1/ Smad pathway. Sci Total Environ, 705: 135-915.

Mackay AL, **1953**. A preliminary examination of the structure of α-$Ca_3(PO_4)_2$. Acta. Crystallogr, 6: 743-744.

Mahajan L, Verma PK, Raina R, Sood S, **2018**. Toxic effects of imidacloprid combined with arsenic: oxidative stress in rat liver. Toxicol Ind Health, 34: 726-735.

Masmoudi S, Larbot A, El Feki H, Amar RB, **2006**. Use of ultrafiltration membranes with apatite for the treatment of cuttlefish effluent. Desalination, 200: 335-336.

Miller LM, Hamerman D, Chance MR, Carlson CS, **1999**. Chemical differences in Subchondral Osteoarthritic Bone observed with Synchrotron Infrared Microspectroscopy. SPIE3775, 104-112.

Mzid M, Badraoui R, Ben Khedir S, Sahnoun Z, Rebai T, **2017**. Protective effect of ethanolic extract of *Urtica urens* L. against the toxicity of imidacloprid on bone remodeling in rats and antioxidant activities. Biomed Pharmacother, 3322: 31073-31079.

Mzid M, Ben Khedir S, Bardaa S, Sahnoun Z, Rebai T, **2017**. Chemical composition, phytochemical constituents, antioxidant and anti-inflammatory activities of *Urtica urens* L. leaves. Arch Physiol Biochem, 123: 93-104.

Nassiri-Asl M, Zamansoltani F, Abbasi E, Daneshi MM, Zangivand AA, **2009**. Effects of *Urtica dioica* extract on lipid profile in hypercholesterolemic rats. J Chin Integr Med, 5: 428-433.

Olszta MJ, Cheng X, Jee SS, Kumar R, Kim YY, Kaufman MJ, Douglas EP, Gower LB, **2007**. Bone structure and formation: A new perspective. Mater Sci Eng R, 58: 77-16.

Radhakrishnan K, Pandi GP, Chandra Mohan S, **2018**. Scanning electron microscopy analysis of effect of *Pedalium murex* (L.) seeds on the morphology of calcium oxalate crystals. Kidney Res J, 8: 1-6.

Randall C, **2003**. Various Therapeutic Uses of *Urtica*. In: *Urtica*: Therapeutic and Nutritional Aspects of Stinging Nettles, Kavalali, G.M. (Ed.). Taylor & Francis, London, UK., 40-46.

Rawi SM, Al-Logmani AS, Hamza RZ, **2019**. Neurological alterations induced by formulated imidacloprid toxicity in Japanese quails. Metab Brain Dis, 34: 443-450.

Raynaud S, Champion E, Bernache-Assollant Dn, **2002**. Calcium phosphate apatites with variable Ca/P atomic ratio I. Synthesis, characterisation and thermal stability of powder. Biomaterials, 23: 1065-1072.

Ronis MJ, Watt J, Pulliam CF, Williams AE, Alund AW, Haque E, Gadupudi GS, Robertson LW, **2019**. Skeletal toxicity resulting from exposure of growing male rats to coplanar PCB 126 is associated with disruption of calcium homeostasis and the GH-IGF-1 axis and direct effects on bone formation. Arch Toxicol, 9.

Sibiya I, Poma G, Cuykx M, Covaci A, Daso AP, Okonkwo J, **2019**. Targeted and non-target screening of persistent organic pollutants and organophosphorus flame retardants in leachate and sediment from landfill sites in Gauteng Province, South Africa. Sci Total Environ, 653: 1231-1239.

Suwalsky M, Orellana P, Avello M, Villena F, **2007**. Protective effect of *Ugni molinae Turcz* against oxidative damage of human erythrocytes. Food Chem Toxicol, 45(1): 130-135.

Suwalsky M, Avello V, Obreque J, Villena F, Szymanska R, Stojakowska A, Strzalka K, **2015**. Protective effect of *Hilesia magellanica* (Coicopihue) from Chilean Patagonia against oxidative damage. J Chil Chem Soc, 60: 2.

Vohra P, Khera KS, Sangha GK, **2014**. Physiological, biochemical and histological alterations induced by administration of imidacloprid in female albino rats. Pestic Biochem Phys, 110: 50-56.

Von Rosenberg S, Wehr U, Bachmann H, **2007**. Effect of vitamin D-containing plant extracts on osteoporotic bone. J Steroid Biochem Mol Biol, 103: 596-600.

Wang H, Chen H, Chernick M, Li D, Ying GG, Yang J, Zheng N, Xie L, Hinton DE, Dong W, **2019**. Selenomethionine exposure affects chondrogenic differentiation and bone formation in Japanese medaka (*Oryzias latipes*). J Hazard Mater, 19: 121-720.

Yashima M, Sakai A, Kamiyama T, Hoshikawa A, **2003**. Crystal structure of β-tricalcium phosphate $Ca_3(PO_4)_2$ by neutron powder diffraction. J Solid State Chem, 175: 272-277.